Accuracy of Myocardial Sodium/Iodide Symporter Gene Expression Imaging with Radioiodide: Evaluation with a Dual-Gene Adenovirus Vector

Kyung-Han Lee, MD[1]; Hye-Kyung Kim, BS[1]; Jin-Young Paik, MS[1]; Takashi Matsui, MD[2]; Yearn Seong Choe, PhD[1]; Yong Choi, PhD[1]; and Byung-Tae Kim, MD[1]

[1]*Department of Nuclear Medicine, Samsung Medical Center, School of Medicine, Sungkyunkwan University, Seoul, Korea; and* [2]*Program in Cardiovascular Gene Therapy, Cardiovascular Research Center, Massachusetts General Hospital, Harvard Medical School, Boston, Massachusetts*

The sodium/iodide symporter (NIS) gene allows convenient reporter imaging with γ-cameras and free radioiodide. In this study, we investigated the accuracy of this technique for assessing myocardial gene expression in living rats by using a dual-gene adenovirus that expresses both NIS protein and enhanced green fluorescent protein (EGFP). **Methods:** Rats underwent myocardial injection with the dual-gene adenovirus (Ad.EGFP.NIS) or a control virus (Ad.EGFP). ^{123}I scintigraphy was performed at day 4, and ratios of cardiac counts to mediastinal count were measured. The site of radiouptake was localized by use of dual-isotope ^{201}Tl images, and radioiodide efflux rates were evaluated by dynamic imaging. The dependence of cardiac radiouptake on viral titers and the sensitivity of detection of cardiac radiouptake were investigated at various viral titers. The radioactivity, EGFP, and NIS protein expression sites were compared microscopically. The correlation of image-based uptake with fluorometric measurements of EGFP concentrations was assessed by regression analysis. **Results:** ^{123}I scintigraphy demonstrated clear focal myocardial uptake at the Ad.EGFP.NIS injection site, with relatively slow washout rates (3.3% ± 0.8%/h), despite the absence of organification. Image-based cardiac uptake increased in a viral titer–dependent manner, with a detection threshold of between 3×10^6 and 1×10^7 plaque-forming units. Western blotting showed titer-dependent increases in myocardial NIS protein expression. Tissue radioactivity levels approached 12.5-fold control levels and correlated closely with image-based uptake ($r = 0.91$; $P < 0.0001$). Histologic analysis confirmed the colocalization of radiouptake, EGFP fluorescence, and NIS staining. Image-based uptake showed a strong correlation with fluorometric measurements of myocardial EGFP concentrations ($r = 0.81$; $P < 0.0001$). **Conclusion:** Our results demonstrate that convenient myocardial gene imaging with γ-cameras and radioiodide is feasible with the NIS gene. Moreover, the use of this technique with a dual-gene vector appears to allow accurate assessment of the level of myocardial expression of a second gene of interest.

Key Words: reporter gene; gene therapy; myocardium; radioiodide; scintigraphy

J Nucl Med 2005; 46:652–657

Because cardiac gene therapy entails multiple complex steps, including the delivery and expression of transgenes (*1,2*), there is an increasing interest in noninvasive methods that allow myocardial gene expression monitoring (*3*). Noninvasive gene imaging can be achieved by exploiting radioprobes that specifically target proteins produced by the transgene of interest. Recently, the use of PET-based myocardial gene imaging in living animals with herpesvirus thymidine kinase or dopamine receptor genes and positron-labeled radioprobes was reported (*4–6*). However, because of the requirement for PET scanners and on-site radiochemical synthesis, widespread use of this method is limited. Therefore, a method that uses more easily accessible instruments and simple radioprobes would significantly benefit the broad application of cardiac gene expression imaging.

The sodium/iodide symporter (NIS), a transmembrane carrier that selectively transports iodide and is the basis for radioiodide thyroid scintigraphy, recently emerged as a convenient and promising reporter for γ-camera imaging of gene expression (*7–12*). In this study, we investigated the accuracy of NIS gene–based radioiodide scintigraphy for noninvasive monitoring of myocardial gene expression in living rats with a dual-gene adenovirus vector that expresses NIS protein and enhanced green fluorescent protein (EGFP) at similar levels.

MATERIALS AND METHODS

Recombinant Adenovirus Vector

Ad.EGFP.NIS contains cytomegalovirus promoter–driven expression cassettes for the EGFP gene and the full-length human

Received Aug. 26, 2004; revision accepted Nov. 17, 2004.

For correspondence or reprints contact: Kyung-Han Lee, MD, Department of Nuclear Medicine, Samsung Medical Center, 50 Ilwondong, Kangnamgu, Seoul, Korea.

E-mail: khnm.lee@samsung.com

NIS complementary DNA (kindly provided by J.-K. Chung, Seoul National University Hospital) substituted for the E1 gene through homologous recombination (*13*). Because this vector system contains dual genes, each with its own promoter and polyadenylation site, 2 separate proteins are produced; the levels of expression of these proteins were previously shown to be similar to each other (*13*). Ad.EGFP, which carries a cytomegalovirus promoter–driven EGFP gene, was used as a control vector. The viruses were amplified in 293 cells, and viral titers were determined by plaque assays.

Rat Myocardial Injection

Sprague–Dawley rats (300–350 g; Charles River Laboratories) were studied under protocols approved by institutional guidelines on the use and care of animals. Rats anesthetized with ketamine (80 mg/kg) and xylazine (10 mg/kg) were mechanically ventilated with room air, and a sternotomy was performed to expose beating hearts. The anterolateral wall of the left ventricle was injected with 3×10^8, 3×10^7, 1×10^7, or 3×10^6 plaque-forming units (pfu) of Ad.EGFP.NIS or 1.5×10^8 pfu of Ad.EGFP in a 100-μL volume with a 30-gauge needle (5 rats per group). Separate animals were used to assess radioiodide efflux rates and to obtain myocardial tissues for Western blotting and microscopic examination.

γ-Camera Imaging of ^{123}I-Injected Rats

For scintigraphic imaging, rats were injected in the tail veins with 74 MBq of $Na^{123}I$ (Korean Atomic Energy Research Center), and $Na^{125}I$ (1.8 MBq) was simultaneously injected to allow γ-counting of explanted tissues at a later time point. Four days after injection was selected as the time for performing scintigraphy because preliminary experiments showed that the intensities of myocardial ^{123}I uptake were almost identical between days 2 and 4 but were no longer visible by day 9. Image acquisition was performed by use of a conventional γ-camera (Monad XLT; Trionix Research Laboratory) with a 20% energy window centered at the energy peak, and images were stored on a 256 × 256 pixel matrix. A lead pinhole collimator with a 5-mm aperture and a focal length of 18 cm was used, and the distance from the pinhole to the rats was approximately 6 cm. Serial image acquisition was performed from 5 min to 200 min after injection in 4 rats to evaluate the myocardial radioiodide efflux rate; a single 45- to 60-min postinjection image was acquired for the remaining animals. Dual-energy acquisition was performed in 2 animals by acquiring myocardial perfusion images 5 min after injection of 18.5 MBq of ^{201}Tl; this step was immediately followed by $Na^{123}I$ injection and image acquisition 45–60 min later as described above.

To semiquantitate the level of myocardial ^{123}I uptake from the images, rectangular regions of interest measuring 5 × 5 pixels were placed on the myocardial region showing increased uptake and on the upper mediastinal region (as background activity); ratios of cardiac counts to mediastinal counts were calculated from these regions of interest. The reproducibility of the quantitation was assessed from data from 3 independent observers, who measured the count ratios 3 separate times. Intraobserver repeatability and interobserver repeatability were expressed as intraclass and interclass correlation coefficients, respectively.

Radioiodide Uptake Measurements in Explanted Hearts

Immediately after the completion of scintigraphic imaging, the animals were sacrificed. The hearts, blood, and major tissues were removed, rinsed clean of blood, and stored at −70°C for 10 d to allow sufficient ^{123}I decay before measurement of ^{125}I radioactivity as the percentage injected dose per gram (%ID/g) of tissue with a γ-counter (Wallac).

To assess the possibility of radioiodide organification, a rat injected with Ad.EGFP.NIS 4 d earlier was injected with 1.85 MBq of $Na^{125}I$ and sacrificed 1 h later. The heart was homogenized in phosphate-buffered saline (PBS) and centrifuged, and the supernatant was loaded into a PD10 gel filtration column (Pharmacia). Fractions of 0.5 mL were eluted with sodium phosphate buffer (0.1 mol/L; pH 7.4) containing 0.1% bovine serum albumin, collected, and counted with the γ-counter. As a control, 37 kBq of $Na^{125}I$ in PBS was analyzed under the same conditions.

Western Blotting for NIS Protein Expression

Membrane preparation and Western blot analysis were performed by a previously described procedure (*14*). In brief, hearts extracted 4 d after viral injection were homogenized in sucrose (250 mmol/L), *N*-(2-hydroxyethyl)piperazine-*N*′-(2-ethanesulfonic acid) (HEPES; 10 mmol/L; pH 7.5), ethylenediaminetetraacetic acid (1 mmol/L), leupeptin (10 μg/mL), aprotinin (10 μg/mL), and phenylmethylsulfonyl fluoride (1 mmol/L) and centrifuged at 5,000*g* and 4°C for 10 min. A 1/10 volume of Na_2CO_3 (1 mol/L) was added to the supernatant, which was then incubated at 4°C for 1 h with continuous shaking. After centrifugation at 75,000*g* and 4°C for 1 h, the pellet was resuspended in a buffer containing sucrose (250 mmol/L), HEPES (10 mmol/L; pH 7.5), and $MgCl_2$ (1 mmol/L). A 20-μg sample of membrane protein was separated on a 12% polyacrylamide gel, electroblotted to a Hybond enhanced chemiluminescence nitrocellulose membrane (Amersham Biosciences), and blocked with 5% dried milk powder in Tris-buffered saline. The membrane was incubated with a mouse monoclonal antibody against human NIS (1:500; Neomarkers) and then with secondary horseradish peroxidase–linked sheep anti–mouse immunoglobulin G (Amersham Biosciences). Enhanced chemiluminescence reagents were used for visualization.

Colocalization of Radioactivity, EGFP Fluorescence, and NIS Staining

A rat myocardium at 4 d after Ad.EGFP.NIS injection was extracted 1 h after $Na^{125}I$ administration, snap frozen, and cryosectioned at a thickness of 10 μm. The sections were air dried after ethanol dehydration and then underwent microautoradiography with a Hypercoat emulsion kit (Amersham Biosciences) according to the manufacturer's instructions. Briefly, the sections were dipped in LM-1 photographic emulsion in a dark room and kept at 4°C and protected from light for adequate durations of exposure. The sections then were sequentially dipped in developer solution, stop solution, and fixer solution, gently washed, and stained with hematoxylin and eosin.

A microscopic section immediately adjacent to that used for microautoradiography was photographed under a fluorescence microscope to localize EGFP expression and then underwent immunostaining to localize NIS protein expression. Briefly, the sections were incubated with an anti–human NIS mouse monoclonal antibody (1:500 dilution, clone FP5A; Lab Vision Corp.) at room temperature overnight and then with biotinylated rabbit anti–mouse immunoglobulin G (DAKO Corp.) for 1 h at room temperature. After horseradish peroxidase–labeled streptavidin was added, diaminobenzidine substrate was applied for color development, and the sections were counterstained with hematoxylin.

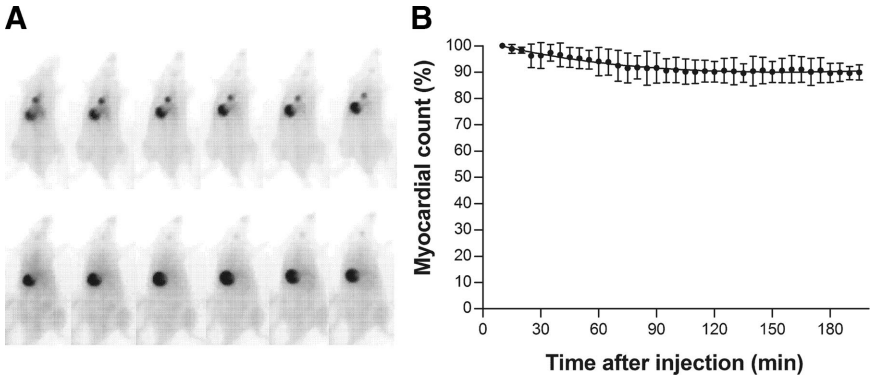

FIGURE 1. (A) Representative serial whole-body ^{123}I images of rats intramyocardially injected with Ad.EGFP.NIS (top) or Ad.EGFP (bottom). Physiologic uptake of free radioiodide can be seen in gastric region and thyroid gland. (B) Time–activity curve for cardiac radioactivity in Ad.EGFP.NIS-injected rats (n = 3), obtained by region-of-interest analysis of images. Myocardial counts corrected for physical decay of ^{123}I are expressed as percentages relative to the value at 5 min.

Fluorometric Quantification of EGFP Expression

Myocardial EGFP expression levels were measured with a fluorometric method previously reported to provide accurate quantification of tissue GFP levels (*15*). Briefly, myocardial tissues were homogenized in PBS and diluted to a protein concentration of 1 mg/mL on the basis of Bradford assays. Volumes of 100 μL were transferred in triplicate to a 96-well plate, and fluorescence was measured with a Magellan fluorometer (TECAN) fitted with 485-nm excitation and 530-nm emission filters according to the manufacturer's instructions. Results were expressed as mean relative fluorescence units for triplicate samples.

Data Analysis

All data are reported as mean ± SD. The significance of differences between groups was evaluated by 1-way ANOVA with Bonferroni's multiple-comparison post hoc tests. Linear correlation was performed to analyze the relationship between image-based uptake levels and fluorometric measurements or γ-counts of explanted tissues.

RESULTS

γ-Camera Imaging with ^{123}I

Serial ^{123}I scintigraphy at 4 d after adenovirus transfer demonstrated focal radiouptake in the cardiac region injected with Ad.EGFP.NIS but not control virus (Fig. 1A). Region-of-interest analysis of cardiac uptake showed an immediate peak, with a relatively slow radioiodide efflux rate of 3.3% ± 0.8%/h (Fig. 1B). When 45- to 60-min ^{123}I images were superimposed on ^{201}Tl myocardial perfusion images obtained by a dual-isotope method in the same rats, the focal area of ^{123}I uptake corresponded to the anterolateral myocardial region consistent with the viral injection site (Fig. 2).

Viral Titer–Dependent Increase in Radioiodide Uptake and NIS Expression

^{123}I images demonstrated intense radiouptake in the myocardial region injected with 3×10^8 pfu of Ad.EGFP.NIS, with a gradual decrease in radiouptake intensity at lower viral titers (Fig. 3). All 5 animals injected with 1×10^7 pfu and 2 of 5 animals injected with 3×10^6 pfu demonstrated discernible focal myocardial uptake.

Measurements of ratios of cardiac counts to mediastinal counts showed good intraobserver reproducibility, with intraclass correlation coefficients of 0.985, 0.991, and 0.986 for the 3 observers. There was also good agreement in ratios between observers, with an interclass correlation coefficient of 0.979. The ratios increased in a viral titer–dependent manner to 364.2% ± 95.1%, 215.5% ± 24.6%, and 161.6% ± 29.9% control levels for groups receiving 3×10^8, 3×10^7, and 1×10^7 pfu, respectively (Fig. 4). For the group receiving 3×10^6 pfu, the 2 animals with a small amount of visible uptake had ratios higher than control levels, whereas the remaining 3 did not. Because cardiac regions of interest include the blood pool, which has higher radioactivity than the mediastinum, the ratios exceeded unity even for control animals.

When homogenized myocardial tissues were subjected to column chromatography, ^{125}I activity coeluted with free radioiodide, indicating the absence of intracellular radioiodide organification. Hepatic ^{125}I uptake values were 0.29 ± 0.19, 0.22 ± 0.08, 0.20 ± 0.06, and 0.17 ± 0.09 %ID/g for rats injected with 3×10^8, 3×10^7, 1×10^7, and 3×10^6 pfu of Ad.EGFP.NIS, respectively, and 0.15 ± 0.03 %ID/g for control rats (P = not significant).

Western blotting of myocardial tissues for NIS protein expression also showed viral titer–dependent band intensi-

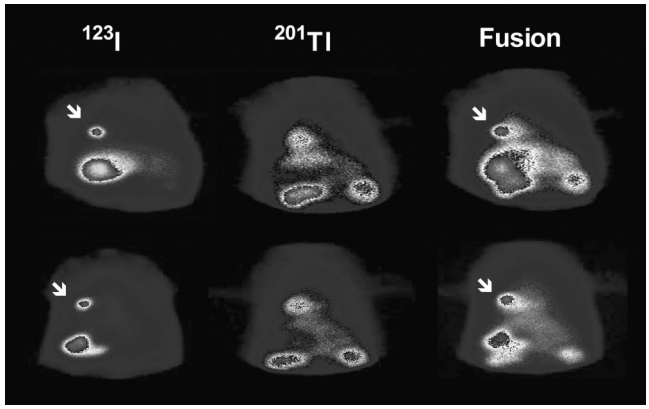

FIGURE 2. Representative ^{201}Tl, ^{123}I, and superimposed scintigraphic images. Superimposed images (right) obtained by overlaying ^{123}I images on ^{201}Tl myocardial perfusion images of same animals indicate ^{123}I activity localized to anterolateral wall region (arrows).

FIGURE 3. ^{123}I scintigraphy of rats intramyocardially injected with Ad.EGFP.NIS. Rats intramyocardially injected with graded Ad.EGFP.NIS titers showed viral titer–dependent myocardial uptake intensities (arrows). All animals injected with 1×10^7 pfu and 2 of 5 animals injected with 3×10^6 pfu had visible myocardial uptake.

ties, with a strong band at 3×10^8 pfu, a moderately intense band at 3×10^7 pfu, and a weak band at 3×10^6 pfu (Fig. 5).

Colocalization of Myocardial EGFP Expression and Radioiodide Uptake

Microautoradiography of a myocardial microsection demonstrated a region of developed silver grains indicated by black coloration corresponding to the presence of radioactivity surrounding a needle track (Fig. 6A). An immediately adjacent microsection demonstrated localized regions of green fluorescence from transgene EGFP expression and an identical distribution of positive immunostaining for human NIS, also surrounding a needle track (Figs. 6B and 6C).

Correlation of Imaging Results with ^{125}I Counts and EGFP Concentrations

Ratios of cardiac counts to mediastinal counts on ^{123}I images showed a high correlation with ^{125}I uptake levels measured by γ-counting ($r = 0.91$; $P < 0.0001$) (Fig. 7A) and with coexpressed EGFP concentrations assessed by fluorometric measurements of explanted myocardial tissues ($r = 0.81$; $P < 0.0001$) (Fig. 7B).

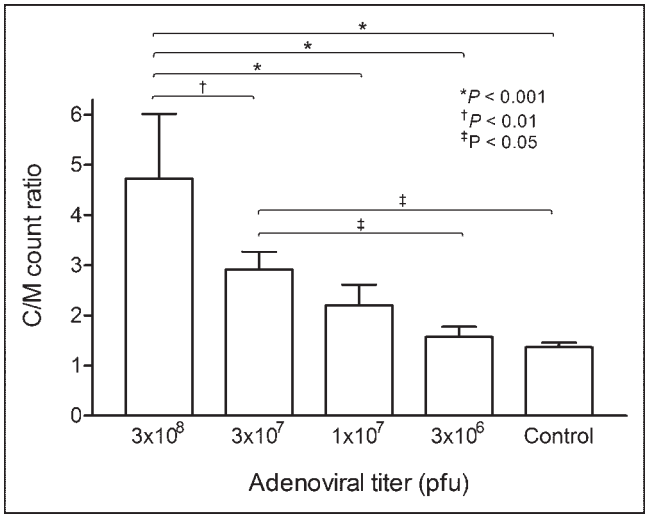

FIGURE 4. Adenovirus titer–dependent myocardial ^{123}I uptake levels assessed from scintigraphic images. Ratios of cardiac ^{123}I counts to mediastinal ^{123}I counts (C/M) were determined by region-of-interest analysis (5 animals per group).

DISCUSSION

In this study, we showed that by use of the NIS gene as a reporter gene, noninvasive myocardial gene expression imaging can be performed with conventional γ-cameras and radioiodide. Scintigraphic images demonstrated focal cardiac radiouptake after injection of Ad.EGFP.NIS but not control virus, a result indicating that radioiodide accumulation is specific for NIS expression. The use of graded viral titers showed a titer-dependent increase in image-based radioiodide uptake levels. All of the animals injected with 1×10^7 pfu and 2 of 5 animals injected with 3×10^6 pfu showed focal myocardial radiouptake. These results indicate a detection sensitivity comparable to that of a previously reported PET-based method (*4*), although it should be noted that the injection dose was slightly larger in our study (74 MBq) than in the PET study (56.5 MBq).

NIS is an intrinsic transmembrane glycoprotein that mediates the active intracellular transport of iodide and sodium. The cloning of the NIS gene has led to a new approach to the imaging of gene expression through transmission of the ability to accumulate radioiodide to nonthyroid tissues by gene transfer (*16*). Transfer of the NIS gene into cell lines enhances radioiodide uptake up to several hundredfold (*17,18*). NIS-expressing tumors also show increased uptake that can be imaged by radioiodide scintigraphy; this technique has been used for various tumor mod-

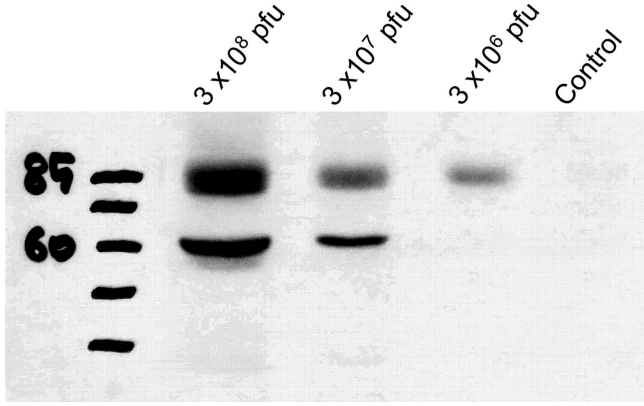

FIGURE 5. Adenovirus titer–dependent myocardial NIS protein expression levels. Myocardial tissues from animals that had been injected with graded Ad.EGFP.NIS titers were analyzed by Western blotting.

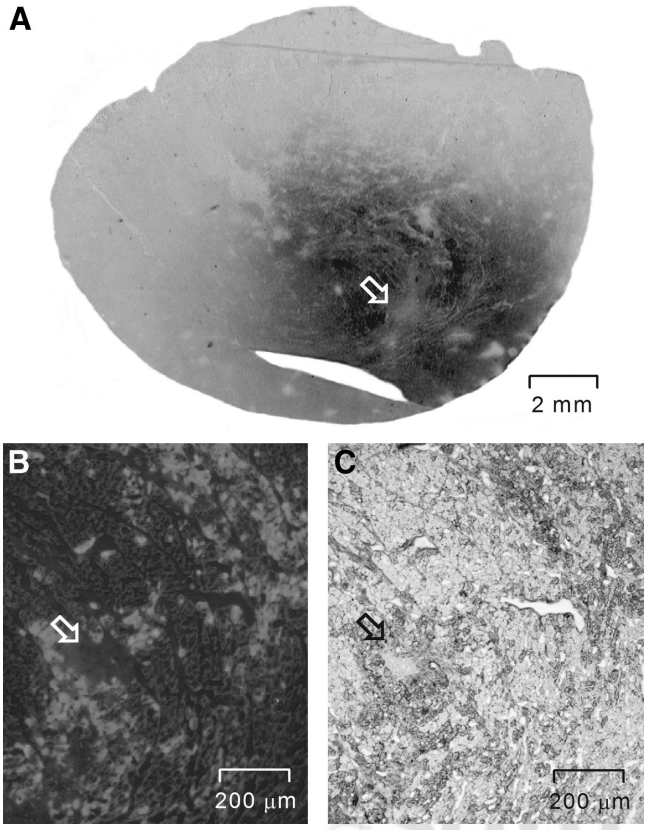

FIGURE 6. Colocalization of radioiodide uptake, EGFP fluorescence, and NIS staining. (A) Microautoradiography of myocardial microsection demonstrates region of dark coloration indicating radiouptake surrounding needle track (arrow). On immediately adjacent microsection, fluorescence microscopy (B) and immunohistochemical analysis (C) demonstrate identical localizations of green fluorescence and NIS staining surrounding needle track (arrows), respectively.

els, including melanoma (*19*), cervical and breast carcinomas (*17*), and prostatic carcinoma (*14*).

These findings have led to the use of NIS as a reporter system for noninvasive gene expression imaging (*7–9*). Groot-Wassink et al. injected mice intravenously with an adenovirus vector; they observed NIS-mediated radioiodide uptake in the liver, adrenal gland, lungs, and pancreas and were able to monitor NIS expression by ^{124}I PET (*10*). The expression of the NIS gene transferred to the liver of mice has also been successfully imaged with $^{99m}TcO_4^-$ (*11*). In a more recent study, Yang et al. evaluated the feasibility of imaging adenovirus-mediated NIS expression in the skeletal muscle of rats and showed that $^{99m}TcO_4^-$ scintigraphy allows the monitoring of gene expression in a quantitative manner (*12*). Our study confirms that the NIS gene is an effective reporter gene for the imaging of gene expression in the myocardium as well.

A potential limitation of the use of the NIS gene for reporter gene imaging is that most nonthyroid tissues do not organify iodide and show rapid efflux of radioiodide after initial uptake. Haberkorn et al. observed that NIS-expressing rat prostate carcinomas retained radioiodide at only 0.4% ID/g after 24 h (*18*). Similarly, Nakamoto et al. found less than 1% of the injected activity in NIS-expressing mammary tumors at 24 h after radioiodide injection, with a calculated biologic half-life of 3.6 h (*20*). A significant rate of radioiodide efflux has also been observed in the livers of mice intravenously administered adenovirus expressing NIS (*10*). In our study, the rate of washout of radioiodide from the myocardium after rapid initial uptake was relatively slow, with a biologic half-life significantly longer than that reported for other nonthyroid tissues. The mechanism for the higher retention rate in myocardial cells was not clear, but there was no evidence of radioiodide organification.

When we examined the time course of scintigraphic findings in a few rats after myocardial Ad.EGFP.NIS injection, cardiac uptake was high at days 2 and 4 but was no longer visible by day 9. The relatively rapid loss of ^{123}I uptake may be related to the rat host immune response against the human NIS protein, in which case the use of species-specific genes could be beneficial. In a few animals, the liver was also faintly visualized, a result indicating that a small amount of virus leaked during myocardial injection and accumulated in the liver. However, this finding does not appear to have substantially affected the results of our study because none of the animals showed high liver activity and there was no significant difference in hepatic uptake related to viral titer.

Image-based ^{123}I uptake levels strongly correlated with ex vivo ^{125}I activity. A somewhat less-than-perfect correlation is not unexpected because, as previously noted, image anal-

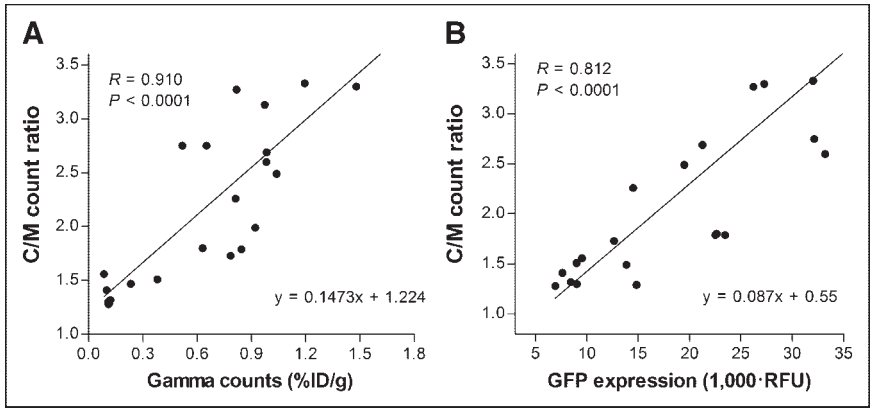

FIGURE 7. Correlation between image-based cardiac uptake levels and ^{125}I counts (A) and fluorometric measurements of EGFP concentrations (B). C/M = ratio of cardiac counts to mediastinal counts; RFU = relative fluorescence units.

ysis was limited to regions of radiouptake, whereas γ-counting was performed for the whole heart (*4*).

Importantly, image-based myocardial radiouptake levels were confirmed to show a strong correlation with fluorometric measurements of concentrations of EGFP, which was coexpressed along with NIS protein by the dual-gene adenovirus vector. Although the rat myocardium emits nonspecific autofluorescence at wavelengths similar to that of GFP, and this autofluorescence can interfere with fluorometric measurements (*21*), EGFP fluoresces 30- to 40-fold brighter than GFP and offers significantly enhanced signal-to-background contrast. Consequently, we were able to show fluorescence intensities up to 6-fold higher in the group receiving Ad.EGFP.NIS than in the control group, and these intensities correlated closely with image-based radiouptake levels. Moreover, myocardial regions that took up radioiodide colocalized perfectly with areas of NIS protein and EGFP expression. These results suggest that this noninvasive technique may provide accurate measurements of transgene expression levels for a different second gene of interest substituted for the EGFP gene.

Recently, PET-based myocardial gene imaging methods were introduced with the herpesvirus thymidine kinase or dopamine receptor gene as the reporter gene (*4*–*6*). PET has the advantage of providing high-resolution, high-sensitivity images with the potential for quantitative measurements. However, the requirement for a PET scanner and a cyclotron facility, which are not readily available in many research laboratories, limits the widespread use of this method. In addition, the short physical half-life of positron emitters necessitates technically demanding on-site radioprobe synthesis by an experienced radiochemist. The use of the NIS gene as a reporter gene provides a much less demanding method for myocardial gene imaging; this method can be performed with easily available γ-cameras and free ^{123}I. This method also permits dual-isotope acquisition for superimposition of radioiodide uptake images on myocardial perfusion images, thereby allowing display of the precise site and extent of gene expression within the myocardium. In addition, the use of species-specific NIS sequences may help circumvent problems arising from the immunogenicity of transgene products.

Limited spatial resolution is a potential drawback of γ-camera scintigraphy in comparison to PET. However, the use of pinhole collimators improves spatial resolution and magnifies areas of interest for small-animal imaging, and single-photon emission tomography techniques can provide tomographic images. Although not investigated in the present study, the NIS reporter system also offers the choice of the use of other radiotracers, such as ^{125}I for imaging with dedicated high-resolution detectors, ^{124}I for PET, and $^{99m}TcO_4^-$, with the added advantages of easy accessibility and low cost.

CONCLUSION

In conclusion, cardiac NIS gene expression can be conveniently monitored in vivo by radioiodide scintigraphy in a sensitive and semiquantitative manner. The use of this technique with a dual-gene vector that includes the NIS gene as a reporter gene may allow accurate monitoring of myocardial expression of a second gene of interest in living subjects.

ACKNOWLEDGMENTS

This work was supported by National Mid- and Long-Term Nuclear R&D Program Grant M20243010001-04A0701-00110 from the Korean Ministry of Science and Technology. The authors are grateful to Dr. Anthony Rosenzweig for invaluable discussion and guidance. This work was presented in part at the 51st Annual Meeting of the Society of Nuclear Medicine, Philadelphia, PA, June 19–23, 2004.

REFERENCES

1. Isner JM. Myocardial gene therapy. *Nature*. 2002;415:234–239.
2. Nabel EG. Gene therapy for cardiovascular disease. *Circulation*. 1995;91:541–548.
3. Avril N, Bengel FM. Defining the success of cardiac gene therapy: how can nuclear imaging contribute? *Eur J Nucl Med Mol Imaging*. 2003;30:757–771.
4. Inubushi MI, Wu JC, Gambhir SS, et al. Positron-emission tomography reporter gene expression imaging in rat myocardium. *Circulation*. 2003;107:326–332.
5. Bengel FM, Anton M, Richter T, et al. Noninvasive imaging of transgene expression by use of positron emission tomography in a pig model of myocardial gene transfer. *Circulation*. 2003;108:2127–2133.
6. Chen IY, Wu JC, Min JJ, et al. Micro-positron emission tomography imaging of cardiac gene expression in rats using bicistronic adenoviral vector-mediated gene delivery. *Circulation*. 2004;109:1415–1420.
7. Dadachova E, Carrasco N. The Na+/I symporter (NIS): imaging and therapeutic applications. *Semin Nucl Med*. 2004;1:23–31.
8. Cho JY. A transporter gene (sodium iodide symporter) for dual purposes in gene therapy: imaging and therapy. *Curr Gene Ther*. 2002;2:393–402.
9. Chung JK. Sodium iodide symporter: its role in nuclear medicine. *J Nucl Med*. 2002;43:1188–1200.
10. Groot-Wassink T, Aboagye EO, Glaser M, et al. Adenovirus biodistribution and noninvasive imaging of gene expression in vivo by positron emission tomography using human sodium/iodide symporter as reporter gene. *Hum Gene Ther*. 2002;13:1723–1735.
11. Lee WW, Moon DH, Park SY, Jin J, Kim SJ, Lee H. Imaging of adenovirus-mediated expression of human sodium iodide symporter gene by $^{99m}TcO_4$ scintigraphy in mice. *Nucl Med Biol*. 2004;31:31–40.
12. Yang HS, Lee H, Kim SJ, et al. Imaging of human sodium-iodide symporter gene expression mediated by recombinant adenovirus in skeletal muscle of living rats. *Eur J Nucl Med Mol Imaging*. 2004;31:1304–1311.
13. He T, Zhou S, da Costa L, et al. A simplified system for generating recombinant adenoviruses. *Proc Natl Acad Sci USA*. 1998;95:2509–2514.
14. Spitweg C, Zhang S, Bergert ER, et al. Prostate-specific antigen (PSA) promoter-driven androgen-inducible expression of sodium iodide symporter in prostate cancer cell lines. *Cancer Res*. 1999;59:2136–2141.
15. Remans T, Shenk PM, Manners JM, et al. A protocol for the fluorometric quantification of mGFP5-ER and sGFP(S65T) in transgenic plants. *Plant Mol Biol Rep*. 1999;17:385–395.
16. Riedel C, Dohan O, De la Vieja A, et al. Journey of the iodide transporter NIS: from its molecular identification to its clinical role in cancer. *Trends Biochem Sci*. 2001;26:490–496.
17. Boland A, Ricard M, Opolon P, et al. Adenovirus-mediated transfer of the thyroid sodium/iodide symporter gene into tumors for a targeted radiotherapy. *Cancer Res*. 2000;60:3484–3492.
18. Haberkorn U, Kinscherf R, Kissel M, et al. Enhanced iodide transport after transfer of the human sodium iodide symporter gene is associated with lack of retention and low absorbed dose. *Gene Ther*. 2003;10:774–780.
19. Mandell RB, Mandell LZ, Link CJ Jr. Radioisotope concentrator gene therapy using the sodium/iodide symporter gene. *Cancer Res*. 1999;59:661–668.
20. Nakamoto Y, Saga T, Misaki T, et al. Establishment and characterization of a breast cancer cell line expressing Na/I symporters for radioiodide concentrator gene therapy. *J Nucl Med*. 2000;41:1989–1904.
21. Kawada T, Shin WS, Nakatsuru Y, et al. Precise identification of gene products in hearts after in vivo gene transfection, using Sendai virus-coated proteoliposomes. *Biochem Biophys Res Commun*. 1999;259:408–413.